DALTON

X-Ray diffraction and solid-state nuclear magnetic resonance study of a silicate containing two different nitrogenous cations

Robin K. Harris,*† Dmitry Yu. Naumov and Abdolraouf Samadi-Maybodi

Chemistry Department, University of Durham, South Road, Durham DH1 3LE, UK

Single-crystal X-ray diffraction has been used to determine the structure of a silicate hydrate containing both the tetraethylammonium cation and a cation containing three nitrogen atoms. The structure is monoclinic, space group $C2/c$, and may be regarded as a host–guest system, with the cations as guests in a hydrogen-bonded framework consisting of a cubic octameric silicate anion, $[Si_8O_{20}]^{8-}$, and water molecules. Magic-angle spinning ^{13}C, ^{29}Si and ^{1}H NMR spectra are consistent with the crystallographic asymmetric unit. The precursor solution, the mother-liquor after crystallisation, and the solution obtained by melting the crystals have also been examined by NMR spectroscopy. The implications for silicate solution equilibria and for zeolite synthesis mechanisms are discussed.

The synthesis of zeolites involves complex chemistry, and the nature of the zeolites formed depends sensitively on the precise constitution of the precursor solutions. These precursors contain silicate, aluminate and aluminosilicate anions with various cations (generally including substituted ammonium ions or related species, which are considered to act as templates) in an alkaline aqueous medium. Even in the absence of any aluminium, such solutions are known to contain a wide range of silicate anions in dynamic equilibria.[1] However, one or two cage-like species generally dominate for alkylammonium silicate solutions,[2] specifically the so-called prismatic hexamer ($Si_6O_{15}^{6-}$ and its congeners) and/or the cubic octamer (the various protonated forms of $Si_8O_{20}^{8-}$). Conceivably, the existence of such species may relate to the mechanism of zeolite formation. In some situations it proves feasible to isolate stable crystalline compounds from these solutions. Recent work[3–8] has shown that these compounds can be regarded as hydrogen-bonded networks of silicate anions and water molecules, with the nitrogenous cations as guests. Thus far, the crystal structures of six such compounds have been reported. Three of these contain singly charged cations, two have doubly charged cations and one has triply charged cations. The silicate–water framework contains the cubic octameric anion (sometimes apparently partially protonated) and variable numbers of water molecules (in some cases disordered in crystallographic sites). Such systems may therefore be considered as examples of host–guest phenomena. It seems that the silicate–water framework can adjust to incorporate cations of different sizes and charges. The variety of structures suggests there may be a relationship with the wide range of zeolites formed by different templates. It therefore appears to us to be important to expand the number of known silicate host–guest systems, which may provide clues to zeolite synthesis mechanisms as well as being of interest in their own right.

In this article we report the first example of such a structure involving two different nitrogenous templates, of importance because zeolite synthesis mixtures sometimes contain more than one type of organic cation. The cations in question are tetraethylammonium and 2,3,4,5,6,7,8,9-octahydro-2,2,5,5,8,8-hexamethyl-2*H*-benzo[1,2-*c*:3,4-*c*′:5,6-*c*″]tripyrrolium (hmbtp), the latter being a triply charged species which has been used[9,10] in the synthesis of zeolites ZSM-18 and SUZ-9. We have recently published[8] a crystal structure of a hmbtp silicate containing the cubic octameric anion in the form $[Si_8O_{18}(OH)_2]^{6-}$ with 41 water molecules. The crystalline silicate we discuss herein can be formulated as $[hmbtp]_2[NEt_4]_2[Si_8O_{20}]\cdot 70H_2O$ **1**, and we have determined its structure by single-crystal X-ray diffraction, supported by ^{29}Si, ^{13}C and ^{1}H magic-angle spinning (MAS) NMR spectra. In order to appreciate more fully the crystallisation process we have also used NMR spectroscopy to examine the precursor solution, the mother-liquor remaining after crystallisation, and the solution obtained by melting **1**.

Experimental

To prepare hmbtp hydroxide, the bromide was first synthesised by the method of Ciric *et al.*[11] and then ion-exchanged.[8] The silicate crystal of $[hmbtp]_2[NEt_4]_2[Si_8O_{20}]\cdot 70H_2O$ **1** was obtained by crystallisation at *ca.* 285 K from an aqueous hmbtp–NEt_4 silicate solution with a silica : cation molar ratio of 1 : 1 and hmbtp : NEt_4 molar ratio of 1 : 6. Since the crystals slowly dehydrate/decompose in air, they were stored under the mother-liquor in a polyethylene container. Such dehydration renders powder XRD measurements inappropriate and complicates the determination of meaningful analytical data. However, as discussed below, single-crystal diffraction experiments were conducted at low temperature and MAS NMR spectra acquired using an enclosed sample.

Crystallography

An appropriate single crystal of approximate size 0.40 × 0.25 × 0.20 mm was mounted on a Rigaku AFC6S diffractometer at 150 K equipped with graphite-crystal-monochromatised Cu-Kα radiation (λ = 1.54178 Å). The structure was initially solved by direct methods (SHELXS 86)[12] and completed by full-matrix least-squares refinement with F_o^2 (SHELXL 93)[13] and Fourier-difference synthesis. A total of

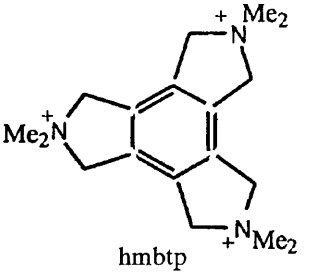

hmbtp

† Fax: 0191 386 1127; E-Mail: r.k.harris@durham.ac.uk

Table 1 Crystal data and structure refinement for compound **1**

Chemical formula	$C_{52}H_{100}N_8O_{20}Si_8 \cdot 70H_2O$
M	2643.24
Crystal system	Monoclinic
Space group	$C2/c$
a/Å	23.730(5)
b/Å	26.280(5)
c/Å	23.570(5)
β/°	111.39(3)
U/Å^3	13 686(5)
Z	4
D_c/g cm^{-3}	1.283
μ/mm^{-1}	1.676
F(000)	5760
θ Range for data collection/°	3.36–75
hkl Ranges	0–29, 0–32, −29 to 27
Reflections collected	12 567
Independent reflections (R_{int})	12 242 (0.0855)
Absorption correction	Semiempirical from ψ scans
Maximum, minimum transmission	1.0000, 0.8823
Refinement method	Full-matrix least squares on F^2
Data, restraints, parameters	12 191, 0, 735
Goodness of fit on F^2	1.020
Final R indices [$I > 2\sigma(I)$]	$R1 = 0.0871$, $wR2 = 0.2287$
(all data)	$R1 = 0.1886$, $wR2 = 0.3255$
Largest difference peak and hole/ e Å^{-3}	0.797, −1.288

12242 independent reflections was used. The hydrogen atoms of the cations were fixed in chemically reasonable positions relative to the heavy atoms during the refinement, but those of the water molecules were not included. Further details of the structure analysis are listed in Table 1.

Atomic coordinates, thermal parameters, and bond lengths and angles have been deposited at the Cambridge Crystallographic Data Centre (CCDC). See Instructions for Authors, *J. Chem. Soc., Dalton Trans.*, 1996, Issue 1. Any request to the CCDC for this material should quote the full literature citation and the reference number 186/159.

NMR measurements

Solid-state ^{13}C and ^{29}Si cross polarisation (CP) MAS NMR spectra of compound **1** were recorded using a Varian Unity Plus spectrometer (7.05 T) at resonance frequencies of 75.43 (^{13}C) and 59.83 MHz (^{29}Si), with spinning rates of 2.45 (^{13}C) and 2.50 kHz (^{29}Si). Also, ^{13}C MAS NMR spectra were recorded with direct polarisation by applying single-pulse excitation and the ^1H MAS NMR spectrum at 299.95 MHz and 2.6 kHz spin rate was also obtained with single-pulse excitation. Chemical shifts of all nuclei are referred to tetramethylsilane. The crystals were first dried between filter-papers and packed into a rotor (outside diameter 7.0 mm).

Spectra for the precursor solution, for the mother-liquor after crystallisation, and for the melt from the crystals (each incorporating 15% w/w D_2O to give a ^2H field/frequency lock signal) were recorded at *ca.* 353 K, at ambient probe temperature (*ca.* 298 K) and at 353 K, respectively, using a Bruker AC250 spectrometer (5.86 T) operating at 49.69 and 62.85 MHz for ^{29}Si and ^{13}C respectively.

Results and Discussion

Crystal structure

Compound **1** crystallises in the monoclinic system, with space group $C2/c$. The asymmetric unit of the structure comprises one NEt_4 and one hmbtp cation (both in general positions), part of an anion (*i.e.* four silicon atoms, four terminal oxygen atoms and seven bridging oxygen atoms, two of which lie on a two-fold symmetry axis), 34 water molecules in general positions and two on two-fold axes, thus giving four formula units of

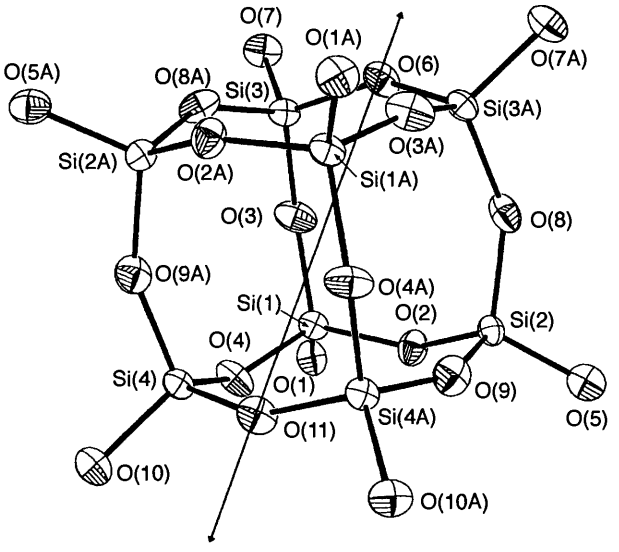

Fig. 1 The double four-ring $[Si_8O_{20}]^{8-}$ anion in $[hmbtp]_2[NEt_4]_2[Si_8O_{20}] \cdot 70H_2O$ at 150 K. The two-fold symmetry axis passing through O(6) and O(11) is indicated

$[hmbtp]_2[NEt_4]_2[Si_8O_{20}] \cdot 70H_2O$ per unit cell. According to the previous discussions[3–8] of analogous crystalline silicates, the crystal structure of **1** may be described as a host–guest compound. The description of the host framework is best started from an idealised three-dimensional, four-connected tetrahedral network in which the tetrahedral positions are occupied by the Si and O_{term} atoms of the octameric double-ring anions and water oxygen atoms (O_w), while the oxygen bridge (O_{br}) atoms are two-co-ordinate. However, apparently some O_w atoms have co-ordination to different numbers of oxygen atoms (see below).

General crystal data are listed in Table 1, bond lengths and angles for the cations and anions in Tables 2 and 3 respectively, and selected interatomic distances and angles in Table 4.

The host structure of the heteronetwork clathrate consists of a three-dimensional assembly of oligomeric $[Si_8O_{20}]^{8-}$ anions and H_2O molecules (O_w) which are linked through hydrogen bonds O–H · · · O. Fig. 1 shows the double four-ring structure of the $[Si_8O_{20}]^{8-}$ anions while Fig. 2 presents a view of the silicate anion surrounded by water molecules. As shown in these figures, the anions are built up of eight SiO_4 tetrahedra sharing three corners each. Each terminal oxygen is strongly hydrogen bonded to three water molecules. The local environment of a silicate anion within the water framework, together with nearby hmbtp and NEt_4 cations, is shown in Fig. 3. Fig. 4 illustrates the crystal structure without the water framework, confirming that the mole ratio of the two cations is 1:1. This view is taken by projection onto the (22$\bar{1}$) plane, which contains a high concentration of ions, forming a pseudo-layer. Two types of cages are present in the heterogeneous network of $[hmbtp]_2[NEt_4]_2[Si_8O_{20}] \cdot 70H_2O$ formed by the host structure. These cages are occupied by hmbtp and NEt_4 cations as guest species, with different orientations, in conformity with the space group (see Fig. 4). The approximate positions of the guest cations within the large polyhedral cavities are shown in Figs. 5 and 6 respectively, while Fig. 7 shows the labelling of both cations, as given in Tables 2 and 3. The orientation of the cationic guest species within the different large polyhedral cavities of the various nitrogen-containing crystalline octameric silicates might be expected to vary with the composition of the homogeneous/heterogeneous networks, *i.e.* the orientation of the cations depends on weak guest–host interactions. Compound **1** is a more water-rich member of the silicate clathrate series than the previous one we have studied[8] (involving hmbtp as the only organic cation). It is closely related

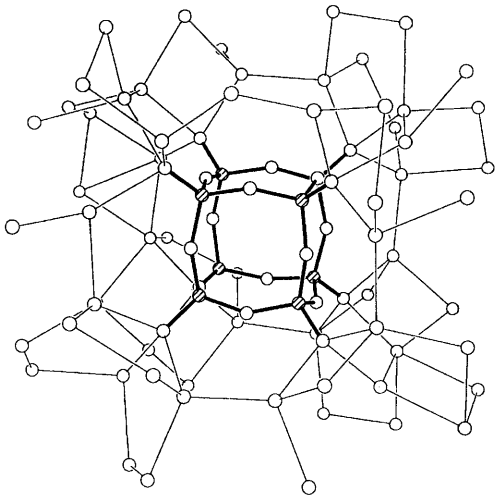

Fig. 2 The double four-ring $[Si_8O_{20}]^{8-}$ anion with its local environment of water molecules. Thick lines represent covalent-ionic bonds Si–O, and thin lines show contacts between donor and acceptor atoms in hydrogen bonds O–H · · · O

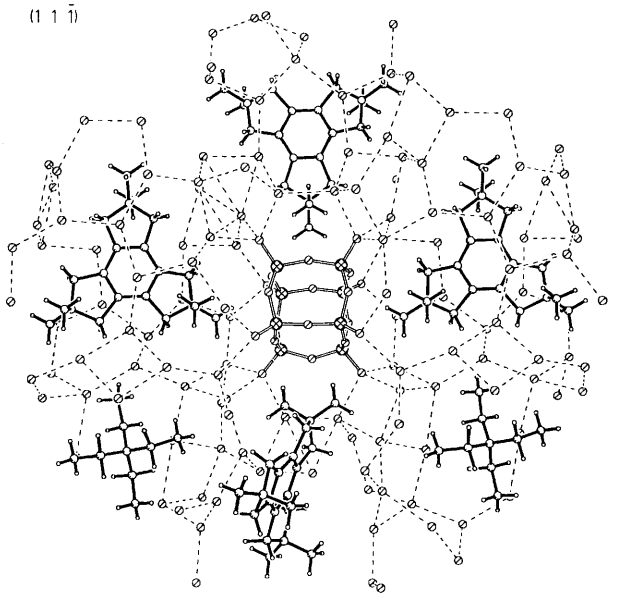

Fig. 3 The double four-ring $[Si_8O_{20}]^{8-}$ anion in $[hmbtp]_2[NEt_4]_2[Si_8O_{20}]\cdot 70H_2O$ with its local environment of water molecules and cations. The anion has site symmetry 2. Double lines represent covalent-ionic bonds Si–O, while dashed lines show contacts between donor and acceptor atoms in hydrogen bonds O–H · · · O. The hmbtp and NEt_4 cations are shown with thick lines

to the many clathrate-hydrate-type phases which have recently been discovered in the system NMe_4OH–water.[14,15]

The geometrical parameters of the silicate anions are typical (Table 4). The double four-ring anions possess a small distortion (site symmetry 2) with regard to the maximum possible point symmetry $m\bar{3}m$ (O_h). The cations surrounding the silicate anion are oriented in such a way that methyl groups point approximately to the anion (Fig. 3).

The environments of each terminal oxygen (O_{term}) and of each water oxygen (O_w) are listed in Tables 5 and 6 respectively. The terminal oxygen atoms are strongly hydrogen bonded to three water molecules each, with O · · · O distances in the narrow range 2.59–2.69 Å. The anions with their immediately neighbouring water molecules therefore form the most strongly bonded part of the host framework. The O · · · O distances between water molecules are generally significantly longer. The distribution of these distances peaks at 2.75–2.80 Å, as is typical for water interactions. The shortest such distance is 2.677 Å, but

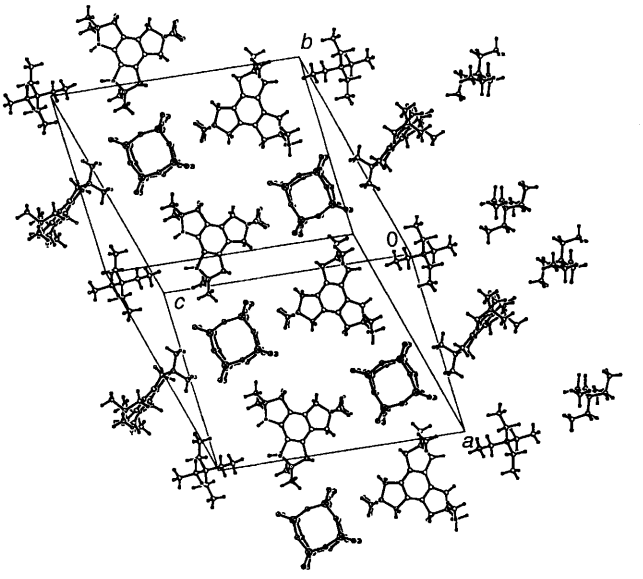

Fig. 4 Packing of cations and anions in the crystal structure of compound **1**: projection onto the (22$\bar{1}$) plane. The water molecules are omitted for clarity

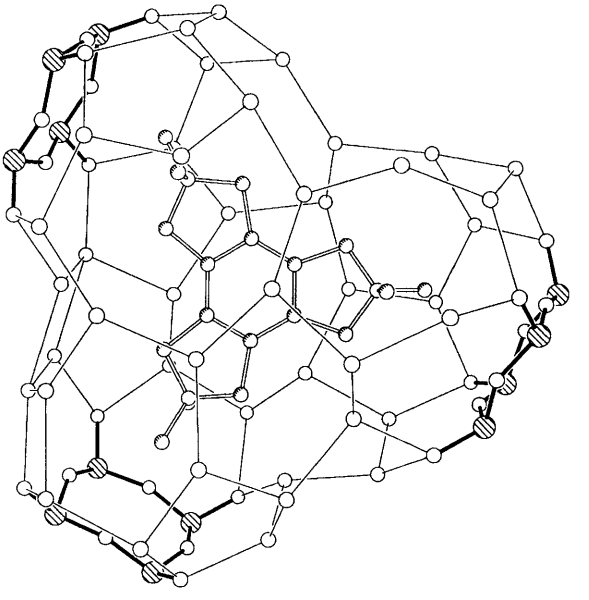

Fig. 5 Cage-like void with the enclosed hmbtp cation. The hmbtp is shown with double lines, thick lines represent covalent bonds Si–O, while thin lines show contacts between donor and acceptor atoms in hydrogen bonds O–H · · · O

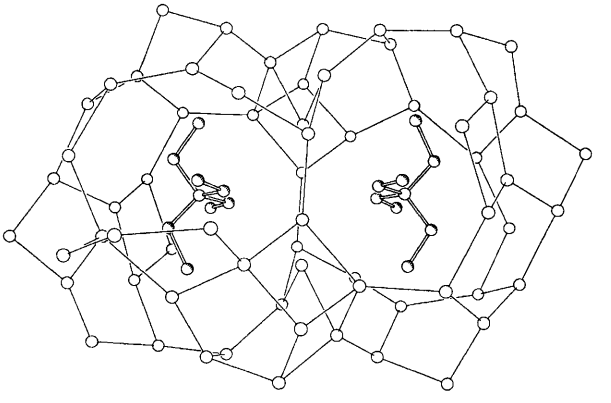

Fig. 6 Cage-like void with the enclosed NEt_4^+ cation. The latter is shown with double lines, while thin lines show contacts between donor and acceptor atoms in hydrogen bonds O–H · · · O

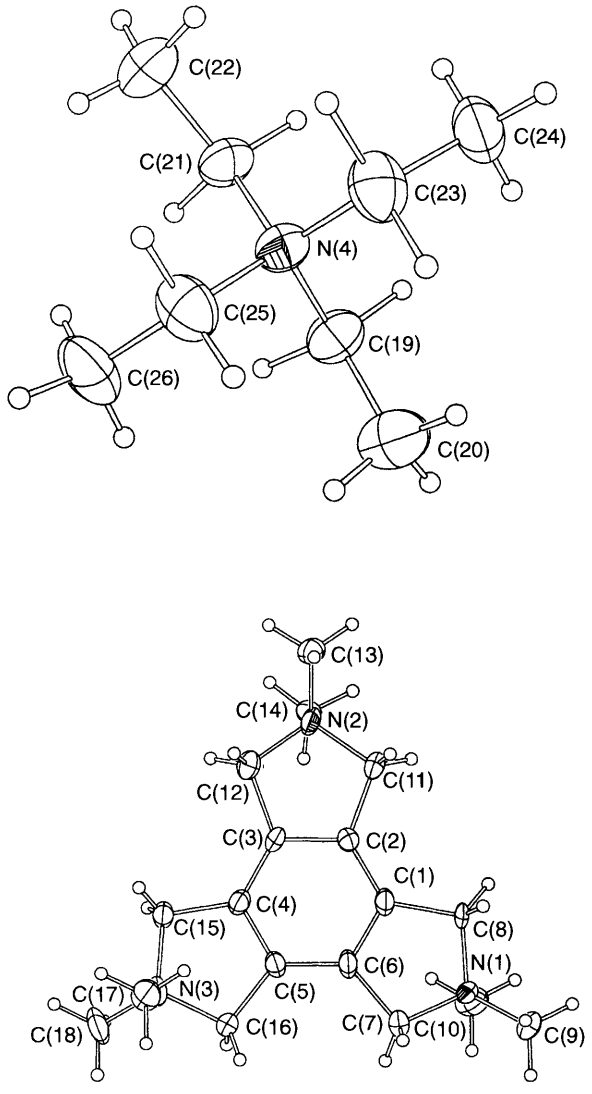

Fig. 7 Cation structures with labelling of carbon and nitrogen atoms. Upper trace: NEt_4^+. Lower trace: hmbtp cation

Table 2 Bond lengths (Å) for the anions and cations of compound **1**

Si(1)–O(1)	1.584(4)	Si(3)–O(7)	1.588(5)
Si(1)–O(3)	1.623(5)	Si(3)–O(3)	1.613(5)
Si(1)–O(2)	1.636(5)	Si(3)–O(6)	1.630(3)
Si(1)–O(4)	1.638(5)	Si(3)–O(8A)	1.635(5)
Si(2)–O(5)	1.586(5)	Si(4)–O(10)	1.594(5)
Si(2)–O(9)	1.624(5)	Si(4)–O(4)	1.622(5)
Si(2)–O(2)	1.624(5)	Si(4)–O(11)	1.623(2)
Si(2)–O(8)	1.628(5)	Si(4)–O(9A)	1.626(5)
N(1)–C(9)	1.491(9)	C(1)–C(2)	1.372(9)
N(1)–C(10)	1.497(10)	C(1)–C(6)	1.387(10)
N(1)–C(7)	1.517(8)	C(1)–C(8)	1.500(8)
N(1)–C(8)	1.535(9)	C(2)–C(3)	1.392(8)
N(2)–C(14)	1.493(10)	C(2)–C(11)	1.506(10)
N(2)–C(13)	1.493(9)	C(3)–C(4)	1.388(10)
N(2)–C(12)	1.522(9)	C(3)–C(12)	1.504(9)
N(2)–C(11)	1.524(8)	C(4)–C(5)	1.387(9)
N(3)–C(17)	1.499(11)	C(4)–C(15)	1.487(9)
N(3)–C(18)	1.502(9)	C(5)–C(6)	1.393(8)
N(3)–C(16)	1.519(8)	C(5)–C(16)	1.498(9)
N(3)–C(15)	1.521(10)	C(6)–C(7)	1.504(9)
N(4)–C(23)	1.510(11)	C(19)–C(20)	1.499(13)
N(4)–C(25)	1.518(11)	C(21)–C(22)	1.529(13)
N(4)–C(21)	1.518(11)	C(23)–C(24)	1.536(13)
N(4)–C(19)	1.542(11)	C(25)–C(26)	1.522(13)

Symmetry transformation used to generate equivalent atoms (see Fig. 1): A $-x + 1, y, -z + \frac{3}{2}$.

Table 3 Bond angles (°) for the anions and cations of compound **1**

O(1)–Si(1)–O(3)	111.6(3)	O(7)–Si(3)–O(3)	110.9(3)
O(1)–Si(1)–O(2)	109.9(3)	O(7)–Si(3)–O(6)	110.3(3)
O(3)–Si(1)–O(2)	108.7(3)	O(3)–Si(3)–O(6)	107.8(2)
O(1)–Si(1)–O(4)	110.8(2)	O(7)–Si(3)–O(8A)	110.5(3)
O(3)–Si(1)–O(4)	108.0(3)	O(3)–Si(3)–O(8A)	108.8(3)
O(2)–Si(1)–O(4)	107.8(2)	O(6)–Si(3)–O(8A)	108.6(2)
O(5)–Si(2)–O(9)	110.3(3)	O(10)–Si(4)–O(4)	108.8(2)
O(5)–Si(2)–O(2)	109.7(2)	O(10)–Si(4)–O(11)	110.7(3)
O(9)–Si(2)–O(2)	108.6(2)	O(4)–Si(4)–O(11)	109.3(2)
O(5)–Si(2)–O(8)	111.8(3)	O(10)–Si(4)–O(9A)	110.8(3)
O(9)–Si(2)–O(8)	108.0(2)	O(4)–Si(4)–O(9A)	108.5(3)
O(2)–Si(2)–O(8)	108.2(3)	O(11)–Si(4)–O(9A)	108.7(2)
Si(2)–O(2)–Si(1)	147.8(3)	Si(2)–O(8)–Si(3A)	148.1(3)
Si(3)–O(3)–Si(1)	160.0(3)	Si(2)–O(9)–Si(4A)	153.0(3)
Si(4)–O(4)–Si(1)	143.7(3)	Si(4)–O(11)–Si(4A)	152.5(4)
Si(3A)–O(6)–Si(3)	143.3(4)		
C(9)–N(1)–C(10)	109.8(6)	C(2)–C(1)–C(6)	119.6(6)
C(9)–N(1)–C(7)	112.3(6)	C(2)–C(1)–C(8)	130.1(6)
C(10)–N(1)–C(7)	107.9(6)	C(6)–C(1)–C(8)	110.2(6)
C(9)–N(1)–C(8)	111.1(6)	C(1)–C(2)–C(3)	120.4(6)
C(10)–N(1)–C(8)	110.2(6)	C(1)–C(2)–C(11)	129.7(6)
C(7)–N(1)–C(8)	105.3(5)	C(3)–C(2)–C(11)	109.8(6)
C(14)–N(2)–C(13)	109.5(6)	C(4)–C(3)–C(2)	119.8(6)
C(14)–N(2)–C(12)	108.4(5)	C(4)–C(3)–C(12)	130.1(6)
C(13)–N(2)–C(12)	112.3(5)	C(2)–C(3)–C(12)	110.1(6)
C(14)–N(2)–C(11)	109.7(5)	C(5)–C(4)–C(3)	120.0(6)
C(13)–N(2)–C(11)	111.8(5)	C(5)–C(4)–C(15)	110.0(6)
C(12)–N(2)–C(11)	105.1(5)	C(3)–C(4)–C(15)	129.9(6)
C(17)–N(3)–C(18)	109.9(6)	C(4)–C(5)–C(6)	119.3(6)
C(17)–N(3)–C(16)	108.8(6)	C(4)–C(5)–C(16)	111.1(6)
C(18)–N(3)–C(16)	111.5(6)	C(6)–C(5)–C(16)	129.5(6)
C(17)–N(3)–C(15)	108.6(6)	C(1)–C(6)–C(5)	120.6(6)
C(18)–N(3)–C(15)	111.4(6)	C(1)–C(6)–C(7)	110.2(5)
C(16)–N(3)–C(15)	106.5(5)	C(5)–C(6)–C(7)	129.1(6)
C(6)–C(7)–N(1)	103.0(6)	C(25)–N(4)–C(21)	111.4(7)
C(1)–C(8)–N(1)	103.0(5)	C(23)–N(4)–C(19)	112.8(7)
C(2)–C(11)–N(2)	103.5(5)	C(25)–N(4)–C(19)	110.4(7)
C(3)–C(12)–N(2)	103.5(5)	C(21)–N(4)–C(19)	104.1(7)
C(4)–C(15)–N(3)	103.0(5)	C(20)–C(19)–N(4)	113.5(8)
C(5)–C(16)–N(3)	102.1(5)	N(4)–C(21)–C(22)	114.3(8)
C(23)–N(4)–C(25)	106.2(7)	N(4)–C(23)–C(24)	114.2(8)
C(23)–N(4)–C(21)	112.0(7)	N(4)–C(25)–C(26)	114.6(8)

Symmetry transformation used to generate equivalent atoms (see Fig. 1): A $-x + 1, y, -z + \frac{3}{2}$.

Table 4 Geometry data for compound **1** (bond distances in Å, angles in °)

	Average	Range
$Si–O_{br}$	1.626	1.613–1.638
$Si–O_{term}$	1.588	1.584–1.594
$O_{br}–Si–O_{br}$	108.2	107.8–109.3
$O_{br}–Si–O_{term}$	110.5	108.8–111.8
$Si–O_{br}–Si$	149.8	160.0–143.3
$O_w \cdots O_w$	2.804	2.677–3.301
$O_{term} \cdots O_w$	2.650	2.596–2.689

there is a tailing off for the longer values, with just three between 2.9 and 3.1 Å and three others between 3.22 and 3.32 Å. At such distances it is arguable as to whether they constitute a hydrogen bond. It is likely that the constraints of forming cages around the cations force these water molecules apart. If only distances of less than 3.1 Å are accounted as hydrogen bonds, then for the water oxygen atoms in the asymmetric unit there is one [O(44)] with two such bonds only, 13 with three, 21 with four and one [O(28)] with five (these numbers include $O_w \cdots O_{term}$ as well as $O_w \cdots O_w$). However, if all $O \cdots O$ distances of less than 3.32 Å are included, there are 10 water molecules with three, 25 with four, and one with five neighbouring oxygens.

Table 5 Environments of terminal oxygen (O_{term}) atoms in compound **1** (distances in Å)

Atom	
O(1)	O(2A) 2.636(11),* O(3A) 2.653(10),* O(4A) 2.651(10),* O(12A) 2.622(10), O(15A) 2.634(10), O(24A) 2.620(10)
O(5)	O(2A) 2.625(10),* O(8A) 2.662(10),* O(9A) 2.634(10),* O(16A) 2.689(10), O(20A) 2.599(10), O(22A) 2.670(10)
O(7)	O(3A) 2.636(10),* O(6A) 2.640(10),* O(8A) 2.649(10),* O(23A) 2.634(10), O(13A) 2.640(10), O(38A) 2.596(10)
O(10)	O(4A) 2.616(10),* O(11A) 2.648(10),* O(9A) 2.650(10),* O(14A) 2.630(10), O(25A) 2.620(10), O(28A) 2.646(11)

* $O_{term} \cdots O_{br}$.

NMR studies

In contrast to diffraction techniques, NMR spectroscopy monitors the local structure around the relevant atom and can be applied to crystalline, amorphous and liquid samples. Within the last decade, solid-state NMR spectroscopy has been developed into an important tool for the structural characterisation of crystalline and non-crystalline silicates.[16,17] In particular, ^{29}Si NMR spectroscopy has been used to study the structural environment of SiO_4 tetrahedra in solid silicates. On the other hand, liquid-state ^{29}Si NMR studies have provided detailed insights into the constitution of silicate anions in silicate solutions.[1,2] To understand the precursor solution and the silicate structure of compound **1**, ^{29}Si, ^{13}C and ^{1}H NMR spectra were obtained.

***(a)* Solution state.** Silicon-29 NMR spectra of the precursor solution at *ca.* 313 K and of the mother-liquor (*i.e.* the saturated solution after crystallisation) at *ca.* 298 K are shown in Fig. 8(*a*) and (*b*) respectively. They were recorded using a substantial recycle delay (50 s) to obtain quantitative data. It can be seen that a wide range of silicon environments is present in both cases. As usual for alkaline silicate signals, separate bands are visible in Fig. 8 for Q^0, Q^1, $Q^2{}_\Delta$, $Q^2/Q^3{}_\Delta$ and Q^3 sites, where the superscripts give the number of siloxane bridges and the subscript triangle refers to three-membered $(SiO)_3$ rings. Peaks assignable to the individual species Q^0, $Q^1{}_2$, $Q^3{}_2$ and $Q^3{}_6$ (known as the monomer, dimer, cyclic trimer, and prismatic hexamer respectively) are of substantial intensity. The mother-liquor of this compound still contains a substantial amount of the $NEt_4{}^+$ cation (as mentioned above, the precursor silicate solution contained a hmbtp:$NEt_4{}^+$ mole ratio of 1:6, but the silicate crystal has a mole ratio of 1:1). Since $NEt_4{}^+$ stabilises the prismatic hexamer[2] it can be expected that the peak assigned to this species is dominant in this solution. However, the corresponding hmbtp–NEt_4 silicate solution contains little or no cubic octamer anion, $Q^3{}_8$ (peak at δ *ca.* 100) in spite of the fact that a corresponding (Si:cation mole ratio 1:1) hmbtp silicate solution shows an intense signal for this anion. Therefore the distribution of silicate anions in hmbtp–NEt_4 silicate solutions is governed preferentially by the $NEt_4{}^+$ cation rather than the hmbtp cation.

The crystalline compound **1** was later melted and the ^{29}Si NMR spectrum obtained at *ca.* 353 K [Fig. 8(*c*)]. This liquid has a high silicate:water molar ratio of 4:35 and a silica to cation ratio of 2:1 (twice that of the precursor solution). The spectrum shows many species are present, with broad lines (indicating relatively facile exchange) except for the $Q^3{}_6$ and $Q^3{}_8$ peaks (which demonstrates their stability). In contrast to the ^{29}Si NMR spectra shown in Fig. 8(*a*) and 8(*b*), this spectrum shows the presence of the cubic octamer. This probably arises from the higher Si:cation molar ratio and high concentration of silica, which factors play an important role for the stabilisation of cage-like species. Moreover, this composition contains a hmbtp:$NEt_4{}^+$ mole ratio of 1:1, which means the concentration of hmbtp is greater than in the precursor solution or mother-liquor, which would tend to stabilise $Q^3{}_8$.

Table 6 Environment of oxygen of water (O_w) atoms in compound **1** (distances in Å)

Atom	
O(12)	O(1A) 2.622(10), O(4A) 3.441(11), O(12A) 3.262(10), O(28A) 2.734(10), O(28B) 3.045(11)
O(13)	O(21A) 2.803(10), O(7A) 2.640(10), O(15A) 2.739(10), O(34A) 2.718(10)
O(14)	O(10A) 2.630(10), O(35A) 2.776(10), O(14A) 2.788(10), O(27A) 2.740(10)
O(15)	O(1A) 2.634(10), O(13A) 2.739(10), O(17A) 2.802(10), O(36A) 2.773(10)
O(16)	O(5A) 2.689(10), O(18A) 2.888(10), O(25A) 2.781(10), O(37A) 2.790(10)
O(17)	O(27A) 2.833(11), O(28A) 2.787(10), O(15A) 2.802(10)
O(18)	O(16A) 2.888(10), O(26A) 2.716(10), O(29A) 2.830(10), O(33A) 2.850(11)
O(19)	O(32A) 2.812(11), O(37A) 2.846(10), O(34A) 2.760(10)
O(20)	O(5A) 2.599(10), O(8A) 3.467(11), O(21A) 2.763(10), O(26A) 2.677(10), O(38A) 2.712(10)
O(21)	O(13A) 2.803(10), O(20A) 2.763(10), O(39A) 2.760(11), O(38A) 3.301(11)
O(22)	O(5A) 2.670(10), O(24A) 2.772(10), O(39A) 2.780(10), O(40A) 2.748(10)
O(23)	O(7A) 2.634(10), O(41A) 2.707(10), O(26A) 2.719(10)
O(24)	O(1A) 2.620(10), O(22A) 2.772(10), O(36A) 2.852(10), O(47A) 2.700(10)
O(25)	O(16A) 2.781(10), O(42A) 2.764(11), O(10A) 2.620(10), O(35A) 2.791(10)
O(26)	O(18A) 2.716(10), O(20A) 2.677(10), O(23A) 2.719(10), O(34A) 2.745(10)
O(27)	O(17A) 2.833(11), O(14A) 2.740(10), O(45A) 2.943(10)
O(28)	O(17A) 2.787(10), O(42A) 2.837(10), O(4A) 3.329(11), O(10A) 2.646(11), O(12A) 2.734(10), O(12B) 3.045(11)
O(29)	O(43A) 2.807(11), O(18A) 2.830(10), O(32A) 2.769(10), O(40A) 2.856(10)
O(30)	O(40A) 2.685(10), O(34A) 2.774(10), O(37A) 2.741(10)
O(31)	O(35A) 2.779(10), O(36A) 2.752(10), O(45A) 2.734(10)
O(32)	O(19A) 2.812(11), O(33A) 2.810(10), O(29A) 2.769(10), O(41A) 2.763(10)
O(33)	O(32A) 2.810(10), O(47A) 2.761(10), O(18A) 2.850(11)
O(34)	O(13A) 2.718(10), O(19A) 2.760(10), O(26A) 2.745(10), O(30A) 2.774(10)
O(35)	O(14A) 2.776(10), O(25A) 2.791(10), O(31A) 2.779(10), O(44A) 3.226(11)
O(36)	O(15A) 2.773(10), O(24A) 2.852(10), O(31A) 2.752(10), O(44A) 2.886(11)
O(37)	O(19A) 2.846(10), O(40A) 2.749(10), O(16A) 2.790(10), O(30A) 2.741(10)
O(38)	O(8A) 3.395(11), O(20A) 2.712(10), O(7A) 2.596(10), O(21A) 3.301(11), O(38A) 2.773(10)
O(39)	O(21A) 2.760(11), O(22A) 2.780(10), O(45A) 2.685(10)
O(40)	O(30A) 2.685(10), O(37A) 2.749(10), O(22A) 2.748(10), O(29A) 2.856(10)
O(41)	O(23A) 2.707(10), O(23B) 2.707(10), O(32A) 2.763(10), O(32B) 2.763(10)
O(42)	O(25A) 2.764(11), O(28A) 2.837(10), O(44A) 2.838(10), O(47A) 2.762(10)
O(43)	O(29A) 2.807(11), O(46A) 2.769(10), O(29B) 2.807(11), O(46B) 2.769(10)
O(44)	O(42A) 2.838(10), O(35A) 3.226(11), O(36A) 2.886(11)
O(45)	O(27A) 2.943(10), O(31A) 2.734(10), O(39A) 2.685(10), O(46A) 2.864(10)
O(46)	O(43A) 2.769(10), O(45A) 2.864(10), O(47A) 2.980(10)
O(47)	O(33A) 2.761(10), O(24A) 2.700(10), O(42A) 2.762(10), O(46A) 2.980(10)

Fig. 9 displays the ^{13}C NMR spectra of the precursor silicate and mother-liquor solutions of compound **1**. Five separate signals are observed in the spectrum. Those at chemical shifts of δ 7.1 and 52.2 may be ascribed to the CH_3 and CH_2 of NEt_4 respectively, while peaks at δ 55.5, 69.5 and 131.2 are assigned to the CH_3, CH_2 and quaternary carbons of hmbtp respectively. The recycle delay might not be enough for quantitative results. However, the two spectra were recorded under the same

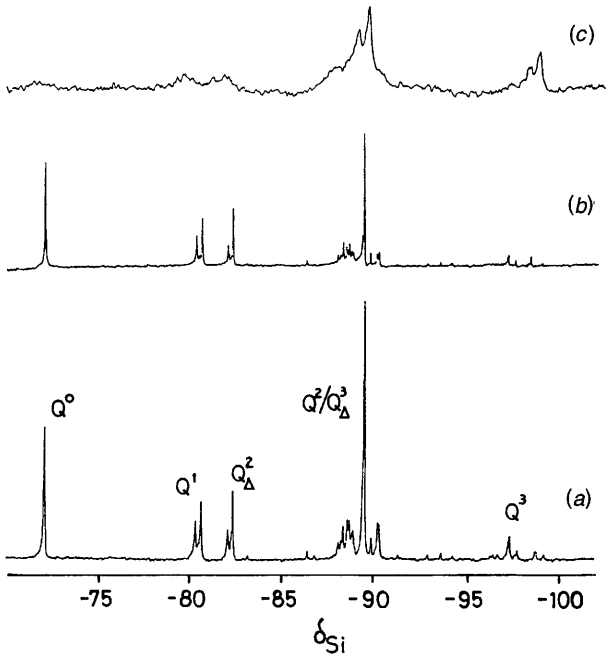

Fig. 8 The 49.69 MHz ^{29}Si NMR spectra of hmbtp–NEt_4 silicate solutions: (*a*) prior to crystallisation at *ca.* 313 K, with 1400 transients; (*b*) the mother-liquor at *ca.* 298 K after crystallisation, with 1300 transients. Spectra (*a*) and (*b*) were recorded under similar conditions: 50 s recycle delay, 4950 Hz total spectral width and 16384 data points. They are plotted on the same scale and with absolute intensity. (*c*) Spectrum of melted $[hmbtp]_2[NEt_4]_2[Si_8O_{20}]\cdot 70H_2O$ at *ca.* 353 K, 45 s recycle delay, 1600 transients, 4950 Hz total spectral width and 16384 data points

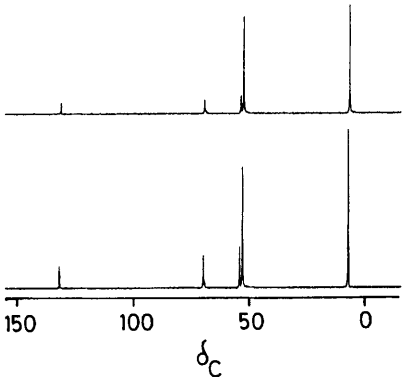

Fig. 9 The 62.85 MHz ^{13}C NMR spectra of hmbtp–NEt_4 silicate solutions. The lower trace shows that of the silicate solution prior to crystallisation at *ca.* 313 K; the upper trace shows that of the mother-liquor at *ca.* 298 K after crystallisation. The two spectra were recorded under similar spectral conditions: 10 s recycle delay, 19230 Hz total spectral width, 16384 data points and 100 transients. They are plotted on the same scale and with absolute intensity

conditions. In general there is no difference between them, except that the NEt_4^+ signals for the mother-liquor are relatively enhanced since, as mentioned earlier, the precursor silicate solution contains a hmbtp:NEt_4^+ mole ratio of 1:6 whereas crystalline compound **1** has a ratio of 1:1 (so that the mother-liquor should contain more NEt_4^+ than the precursor solution).

***(b)* Solid state.** Fig. 10 displays the 59.83 MHz CP MAS ^{29}Si NMR spectrum of the powdered solid **1** at 263 K. Although the crystallographic data indicate there are four independent silicon sites in the double four-membered ring (Table 2), this spectrum shows only two peaks (at chemical shifts δ −98.86 and −99.06 from the signal for $SiMe_4$) indicating that the crystallographic sites can be grouped into only two distinguishable environments. Although the recycle delay of 5 s might not be enough for the

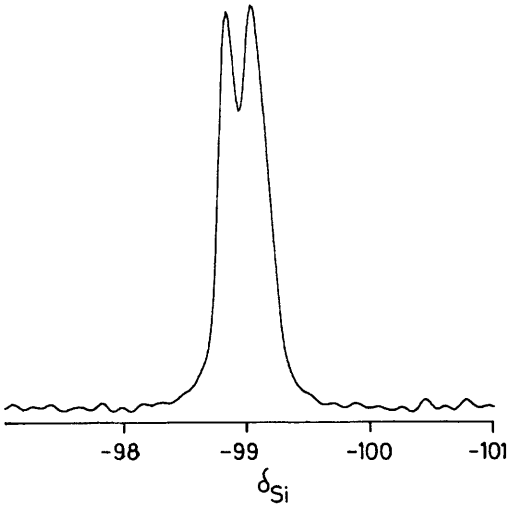

Fig. 10 The 59.83 MHz CP MAS ^{29}Si NMR spectrum of solid compound **1** at 263 K. Spectral parameters: 5 ms contact time, 5 s recycle delay, 240 transients, 30007.5 Hz total spectral width, 32768 data points and 2500 Hz spin rate

quantitative measurement, it seems that the two sites have the same number of silicon atoms, *i.e.* four. This crystal system is more symmetric (monoclinic) than the previous one studied[8] (triclinic), which is consistent with the relatively small shift range. The grouping of signals into two pairs probably reflects the substantial difference in the spread of O_{br}–Si–O_{br} bond angles between Si(1) with Si(3) on the one hand and Si(2) with Si(4) on the other. Thus, the crystallographic data and NMR results are in agreement and it is clear the bulk sample consists of a pure form. The structure-directing property of the organic cation is shown by comparison of the silicon-29 NMR spectra of the precursor solution and of the silicate crystal. Although the former shows little or no signal for the cubic octamer, the crystalline material of this composition (compound **1**) involves only the double four-membered silicate ring.

Fig. 11(*a*) shows the 75.43 MHz CP MAS ^{13}C NMR spectrum of powdered compound **1** at 263 K. Five major bands are seen, as expected, at δ 55.4, 69.5 and 131.12, assignable to the CH_3, CH_2 and quaternary carbon nuclei of hmbtp respectively, and δ 7.1 and 52.2, ascribed to the CH_3 and CH_2 of the NEt_4^+ carbon nuclei respectively. The atomic coordinates of compound **1** indicate there are six different crystallographic sites for each group of carbon atoms (*i.e.* 18 independent carbons) of hmbtp. Although these are not resolved, all peaks show evidence of shoulders and splitting arising from different crystallographic sites.

It is noticeable that, although the crystal structure involves a hmbtp:NEt_4 mole ratio of 1:1, the signal associated with hmbtp [Fig. 11(*a*)] is more intense than that of NEt_4^+, which indicates that the transfer of magnetisation from hydrogen to carbon for the two cations is not the same. To understand this fact the ^{13}C MAS NMR spectrum of compound **1** was recorded [Fig. 11(*b*)] under the same conditions except using direct polarisation rather than cross polarisation. As can be seen, the peak heights of the carbons associated with the NEt_4 cation are now more than those of hmbtp. This fact is consistent with the crystallographic data, which reveal that the cages around the disordered cations of hmbtp and NEt_4 are very different. It seems the NEt_4^+ is more mobile (Fig. 6) than hmbtp (Fig. 5). Both spectra (Fig. 11) display carbon signals associated with NEt_4^+ which are narrower than those for hmbtp, again indicating mobility of NEt_4^+. The considerable linewidths for the hmbtp cation may also, however, arise from dispersion of chemical shifts.

The solid-state ^1H MAS NMR spectrum of compound **1** was obtained at 263 K with single-pulse excitation (Fig. 12). This

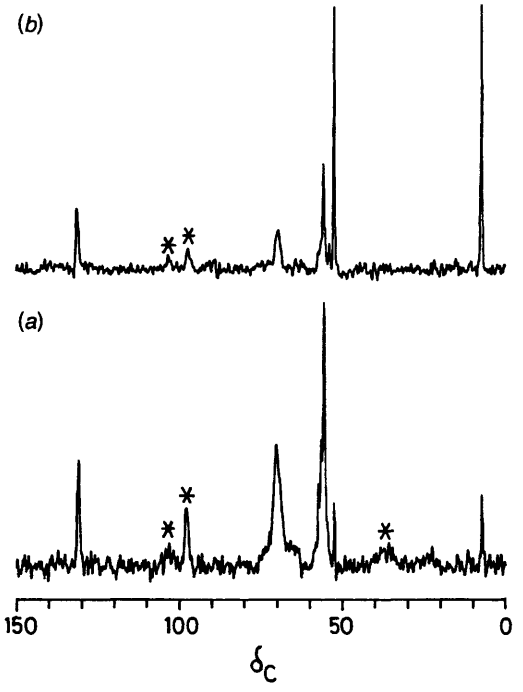

Fig. 11 The 75.43 MHz MAS ^{13}C NMR spectra of solid compound **1** at 263 K: (*a*) with cross polarisation; 5 ms contact time, 5 s recycle delay, 340 transients, 30007.5 Hz total spectral width, 65536 data points and 2450 Hz spin rate; (*b*) with direct polarisation; 160 transients, 30 s recycle delay, 30007.5 Hz total spectral width, 65536 data points and 2600 Hz spin rate. The peaks marked by asterisks are spinning sidebands

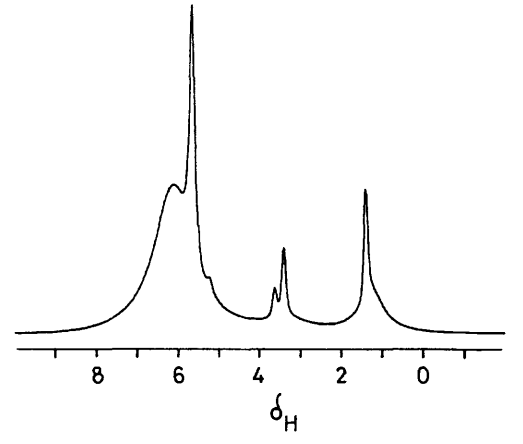

Fig. 12 The 299.95 MHz MAS ^{1}H NMR spectrum of solid compound **1** at 263 K. Spectral parameters: 100 transients, 5 s recycle delay, 100 kHz total spectral width and 2600 Hz spin rate

displays peaks at δ 1.39 and 3.38, assignable to the hydrogen nuclei of the methyl and methylene groups of the NEt_4^+ respectively, and at δ 3.61 and 5.22 which are associated with the hydrogen nuclei of the methyl and methylene groups of the hmbtp cation respectively. There is a broad peak in the range δ *ca.* 5–7, but interestingly there is another narrow peak, of substantial intensity, at δ 5.65 in this spectrum. Presumably there are two kinds of hydrogen nuclei in the water framework of the crystalline material of $[hmbtp]_2[NEt_4]_2[Si_8O_{20}]\cdot 70H_2O$. As explained earlier, the hydrogen bonds to the terminal oxygen atoms O_{term}, *i.e.* $O_{term}\cdots O_w$, are stronger than those of $O_w\cdots O_w$ (Tables 5 and 6). Moreover, there is a wide variety of $O_w\cdots O_w$ distances. Consequently, the broad line can arise from the different environments of the hydrogen nuclei and/or the mobility of the hydrogen atoms of the weak hydrogen bond, whereas the narrow peak might arise from the strong hydrogen bonds. However, such an explanation is speculative.

Conclusion

The crystal structure of $[hmbtp]_2[NEt_4]_2[Si_8O_{20}]\cdot 70H_2O$ is the first to be reported for an organic silicate which has octameric anions and two different organic cations. It supports our recent experimental findings[8] for a related compound as well as other alkylammonium silicate hydrates,[3–7] which have important implications for zeolite chemistry. Detailed investigations into the organisation of silicate species, organic cations and H_2O molecules are of particular interest with regard to questions concerning the mechanisms of zeolite formation. The variety of silicate–water networks now known for nitrogen-containing organic silicates may provide a clue to the existence of so many different zeolite frameworks. At the very least there is a parallel complexity of structure.

It is pertinent that discrete double four-ring species are rare in crystalline metal silicates,[18] but have been found to occur in crystalline silicate hydrates such as **1** and also in various reported hydrated quaternary alkylammonium silicates.[2,19]

Acknowledgements

One of us (A. S.-M.) thanks the Iranian Ministry of Culture and Higher Education for a studentship. D. Y. N. is grateful to the University of Durham for financial backing. We acknowledge support from the UK Engineering and Physical Sciences Research Council for access to the Solid-state NMR Service based at Durham. We are grateful to Dr. A. Batsanov for help with the interpretation of the X-ray diffraction results, to Nicola A. Davies for assistance with the solid-state NMR experiments and to Dr. W. Smith for helpful comments. General support from BP Chemicals Ltd., Sunbury-on-Thames, is gratefully acknowledged.

References

1 R. K. Harris and C. T. G. Knight, *J. Chem. Soc., Faraday Trans. 2*, 1983, 1525, 1539.
2 R. K. Harris and C. T. G. Knight, *J. Mol. Struct.*, 1982, **78**, 273; D. Hoebbel, G. Garzo, G. Engelhardt, R. Ebert, E. Lippmaa and M. Alla, *Z. Anorg. Allg. Chem.*, 1980, **465**, 15; D. Hoebbel, A. Vargha, B. Fahlke and G. Engelhardt, *Z. Anorg. Allg. Chem.*, 1985, **521**, 61.
3 M. Wiebcke, *J. Chem. Soc., Chem. Commun.*, 1991, 1507.
4 M. Wiebcke, M. Grube, H. Koller, G. Engelhardt and J. Felsche, *Microporous Mater.*, 1993, **2**, 55.
5 M. Wiebcke and D. Hoebbel, *J. Chem. Soc., Dalton Trans.*, 1992, 2451.
6 M. Wiebcke, J. Emmer and J. Felsche, *J. Chem. Soc., Chem. Commun.*, 1993, 1604.
7 M. Wiebcke, J. Emmer, J. Felsche, D. Hoebbel and G. Engelhardt, *Z. Anorg. Allg. Chem.*, 1994, **620**, 757.
8 R. K. Harris, J. A. K. Howard, A. Samadi-Maybodi, J. W. Yao and W. Smith, *J. Solid State Chem.*, 1995, **120**, 231.
9 J. Ciric, *U.S. Pat.*, 3 950 496, 1976.
10 W. J. Smith, *Eur. Pat.*, 0 526 252 Al, 1993.
11 J. Ciric, S. L. Lawton, G. T. Kokotailo and G. W. Griffin, *J. Am. Chem. Soc.*, 1978, **100**, 2173.
12 G. M. Sheldrick, SHELXS 86, University of Göttingen, 1986.
13 G. M. Sheldrick, SHELXL 93, University of Göttingen, 1993.
14 D. Mootz and R. Siedel, *J. Inclusion Phenom. Mol. Recognit. Chem.*, 1990, **8**, 139.
15 W. Hesse and M. Jansen, *Z. Anorg. Allg. Chem.*, 1991, **595**, 115.
16 G. Engelhardt and D. Michel, *High Resolution Solid State NMR of Silicates and Zeolites*, Wiley, Chichester, 1987.
17 H. Eckert, *Prog. Nucl. Magn. Reson. Spectrosc.*, 1992, **24**, 159.
18 G. Bisser and F. Liebau, *Z. Kristallogr.*, 1987, **179**, 359.
19 O. Rademacher, O. Ziemens and H. Scheler, *Z. Anorg. Allg. Chem.*, 1984, **519**, 165.

Received 4*th April* 1996; *Paper* 6/02359B